

# Reports

## Diamagnetic Solar-Wind Cavity Discovered behind Moon

**Abstract.** Preliminary Ames-magnetometer data from Explorer 35, the lunar orbiter, show no evidence of a lunar bow shock. However, an increase of the magnetic field by about 1.5 gamma (over the interplanetary value) is evident on Moon's dark side, as well as dips in field strength at the limbs. Interpretation of these spatial variations in the field as deriving from plasma diamagnetism is consistent with a plasma void on the dark side, and steady-state ( $\dot{B} = 0$ ) magnetic transparency of Moon.

Interaction of the solar wind with Moon has been observed by magnetic-field measurements made by the Ames magnetometer aboard the lunar satellite Explorer 35. The data indicate that the interaction is confined mainly to the region in Moon's geometric shadow. The cavity created by obstruction by Moon of the streaming solar wind is frequently detectable magnetically as a field increase by about 1.5 gamma relative to the interplanetary value (1 gamma,  $10^{-5}$  gauss), and the onset of cavity-field increases is preceded and followed by a decrease in field of several gammas. The magnetic signature

of the cavity can be explained as due to the diamagnetism of the solar wind. In addition to these effects connected with the side of Moon away from Sun, preliminary analysis of data from 22 orbits shows no evidence of a lunar bow shock. Consequently the current system generated by the motional electric field is limited; since this limitation may be due to the impedance of the crust, conclusions about the interior bulk electrical conductivity or inferences of an interior temperature still seem premature. This report first considers the satellite orbit and then discusses the magnetometer signature in

the cavity and at its boundaries; finally the consequences of the lack of a signature outside the boundaries are examined.

Explorer 35 was injected into lunar orbit at 0919 universal time on 21 July 1967 while Moon was immersed within the geomagnetic tail structure. The orbital parameters for the first orbit were: semimajor axis,  $3.43 R_m$ ; semiminor axis,  $2.80 R_m$  ( $R_m = 1.74 \times 10^3$  km); period, 11.5 hours; and eccentricity, 0.580. Periselene and aposelene altitudes were 763 and 7670 km, respectively. The angle between the major axis and the ecliptic plane was  $12.7^\circ$ , and the minor axis was canted at an angle of about  $7^\circ$ , with the descending leg of the satellite's orbital motion opposing the direction of Moon's orbital motion. The orbital parameters did not vary significantly for the later orbits we report. Figure 1 shows orbit 20 projected into the ecliptic plane; the portion of the orbit during which the spacecraft is in lunar eclipse is projected into a plane normal to the Moon-Sun line. The spacecraft is spin-stabilized along an axis nearly in the ecliptic north-south direction for the data reported here. Of the three component sensors comprising the field detectors, two are in the spin plane; any offsets due to zero drift in these sensors are removed by a transformation from the rotating to a fixed (inertial) coordinate system. The offset error in the third sensor, which points along the spin axis, is believed to be less than 0.5 gamma, as determined by preflight calibration and by preliminary analysis of inflight calibration data. A small offset in magnitude of this component, if later found to be present, will not affect our major conclusions.

Magnetic-field vector information is given in a spherical coordinate system in which  $\theta$  is the angle of the magnetic vector to the ecliptic plane and  $\phi$  is the angle between the ecliptic projection of the vector and the spacecraft-Sun line (clockwise as viewed from the north). During optical shadow, the view of Sun necessary for fixing the value of  $\phi$  is not available, and memory of the spin period is retained by a pseudo-pulse of the Sun generated on the spacecraft. Values of  $\phi$  during optical shadow periods are not given here; they will be available after analysis of the shadowed spin period.

We center attention on interplanetary-field data acquired after 25 July, when the last outbound crossing of Earth's bow shock is seen; data are

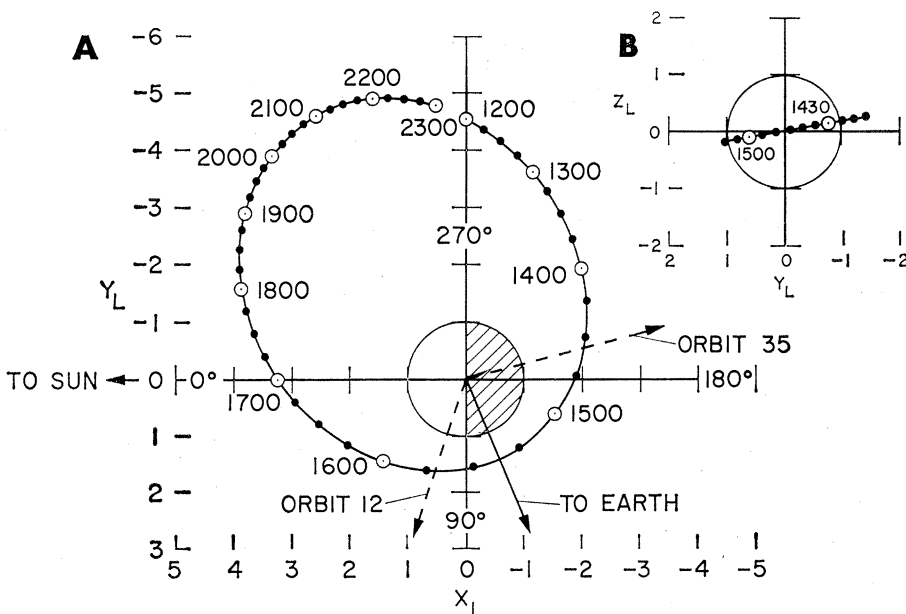


Fig. 1. (A) Course of orbit by Explorer 35 about Moon, projected on the ecliptic plane. The range of directions of the line of sight to Earth for orbits 12 through 35 is shown by dashed lines. The  $+X_L$  axis points along the Moon-Sun line, while  $-Y_L$  is in the direction of Moon's orbital motion around Sun. Time ticks are for every 15 minutes. (B) The dark-side portion of orbit 20 is shown projected on the plane perpendicular to the Moon-Sun line, where  $+Z_L$  is in the ecliptic north direction. Time ticks are at 5-minute intervals.

available, for periods during which the spacecraft is in lunar shadow, for 22 of the next 28 orbits. Five of the orbits have so many gaps in the data that no definite assessment can be made. Fifteen of the remaining 17 passes exhibit characteristic features seen when the satellite passes through Moon's shadow; three examples appear in Fig. 2. First, typically the magnitude of the field in Moon's shadow is increased above the interplanetary value by about 1.5 gamma. Variations of  $\theta$  in Moon's shadow resemble those in the free stream. There is evidence, not shown in Fig. 2, that on one pass the same is true for  $\phi$ .

Figure 2 also shows well-defined local minima in the field-magnitude plots at the boundaries of the cavity: the field strength sometimes decreases to values of less than 1.0 gamma for several individual samples of data (6 seconds apart). The features shown in Fig. 2 are not always seen; two passes are relatively featureless (Fig. 3). The duration of the dips is between 9 and 18 minutes, averaging 13 minutes, for 19 observations at the cavity boundary.

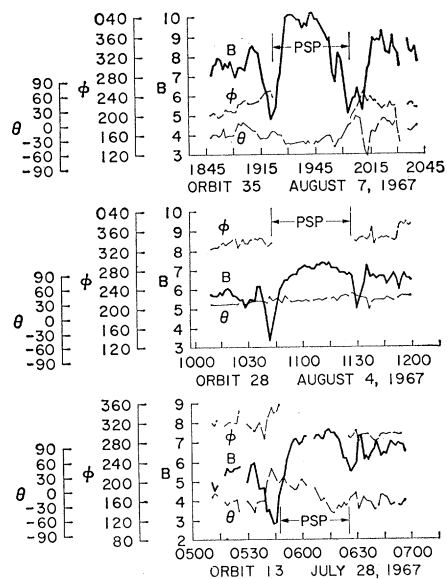


Fig. 2. Magnetic-field data from three passes through Moon's shadow that exhibit effects attributed to diamagnetism of solar-wind plasma (see text);  $B$  is the magnetic-field magnitude,  $\theta$  is the angle between the field vector and the ecliptic plane, and  $\phi$  is the angle between the ecliptic projection of the vector and the spacecraft-Sun line (clockwise as viewed from the north). Data are sequence (81.8-second) averages containing 13 or 14 individual vectors; PSP is the period during which the satellite was in the region shadowed from Sun by Moon. The altitude of the satellite decreases from 1.3 lunar radii at shadow entrance to 0.5 lunar radii at shadow exit.

24 NOVEMBER 1967

Five remaining minima, observed as the spacecraft enters the cavity, are of less than 7 minutes' duration; two of these, of less than 1 minute, are discussed later. If one considers the spacecraft's velocity, an average time of 13 minutes corresponds to a boundary width of 1040 km.

Interception of solar-wind plasma by Moon is expected to create a plasma void behind Moon, since the thermal velocity of solar-wind protons is many times lower than the bulk velocity that carries them past Moon. The axis of symmetry of the resultant cavity is determined by the aberrated direction of the flow of solar wind, and differs from that of Moon's optical shadow. Times when the magnetometer Sun pulse is switched to the pseudo-pulse of the Sun are used to indicate roughly when the cavity boundary is crossed; more refined comparisons can be made when both plasma and magnetic data can be correlated. Plasma diamagnetism could cause the observed increase in field magnitude if the interplanetary magnetic field were otherwise unaffected by Moon, because of the lack within the cavity of gyrating particles that normally so move as to reduce the strength of the magnetic field. Data from the first two periselene passes (when Moon is immersed in Earth's magnetic tail) have yielded (1) a conservative bound of 2 gamma to any intrinsic lunar field at an altitude of 0.5 to 1  $R_m$ ; they show that a hypothetical lunar dipole, oriented along the rotation axis, would have a magnetic moment less than  $7 \times 10^{-6}$  that of Earth.

While an intrinsic magnetic field, distorted by the solar wind, could be comparable in magnitude to the observed increase, its addition to the interplanetary field would usually involve a change in direction that we have not observed; neither would an intrinsic field explain larger increases observed when Moon is behind Earth's bow shock—in one such instance, an increase in field magnitude of 8 gamma.

At the boundary of a cavity, the linear equation of motion for a collisionless plasma reduces to this approximate solution:

$$nk(T_e + T_i) = (B_2^2 - B_1^2)/2\mu_0$$

where  $B_2$  and  $B_1$  are the strengths of magnetic fields of cavity and interplanetary space, respectively;  $n$  is the number density of solar-wind ions;  $T_e$  and  $T_i$  are the temperatures of electrons and ions, respectively;  $k$  is Boltzmann's constant; and  $\mu_0$  is the permea-

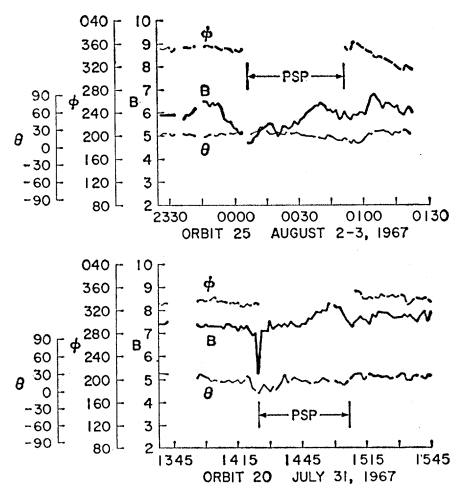


Fig. 3. Same as Fig. 2 for two passes through Moon's shadow with relatively featureless magnetic data.

bility of free space (2). For the more general case having a nonzero component  $B_n$  normal to, and  $B_t$  parallel to, the boundary, the equation of motion is obtained by integrating

$$2B_t dB_t = 2\mu_0 nk(T_e + T_i)\cos \eta dx/x_0$$

where  $x_0$  is the boundary width and  $\eta$  is the angle of the field to the boundary surface. The integral is the equation of motion for a boundary cut by field lines. (Such a boundary cannot be maintained in the steady state in the rest frame of the plasma because of particle motion along field lines that will close the cavity.) The exact integral of the equation is given by

$$B_{t2}B_2 - B_{t1}B_1 + B_n^2 \log \frac{B_{t2} + B_2}{B_{t1} + B_1} = 2\mu_0 nk(T_e + T_i)$$

which may be approximated by

$$B_2^2 - B_1^2 \cong 2\mu_0 nk(T_e + T_i)\cos \bar{\eta}$$

where  $\bar{\eta}$  is a mean value of  $\eta$ . The increase of field within the cavity can be described as resulting from a sheet current at the cavity boundary, caused by the decrease in density of gyrating particles. The equation of motion implies that, for low values of  $\bar{\eta}$ , the ion-particle density across the boundary decreases from 5/cm<sup>3</sup> in the solar wind to zero in the cavity if the magnetic-field strength rises from 5 gamma in the solar wind to 7 gamma in the cavity, and if the sum of electron and ion temperatures is  $1.5 \times 10^5$  °K. For most of the data in this report the interplanetary field has the spiral-angle orientation, so that  $\bar{\eta}$  is about 45°.

Since  $\nabla \cdot \vec{B} = 0$  requires that the total magnetic flux directed inward

across any closed surface must equal that directed outward, local regions of enhanced field strength, in an otherwise uniform field, must be accompanied by neighboring regions of depression of field intensity. The solution for a high-permeability cylinder in a uniform transverse field (3) shows an exterior dip as great as the increase in field in the interior of the cylinder. The case of Moon's cavity is more complicated because the super-Alfvénic flow prevents the dip from extending farther than the confines of the magnetoacoustic Mach angle, which is typically small. Nevertheless the field lines of the surface currents, which close upon themselves, must depress the field outside the cavity as well as increase the field inside.

Explanation of the boundary dips is apparent if one postulates a plasma layer having an increased density-temperature product at the boundary. We consider two limiting cases, with the field direction primarily in the boundary direction ( $B_n = 0$ ) or alternatively perpendicular to the boundary plane ( $B_t = 0$ ): In the former case, if the boundary is created by an increased product  $nT$  near the limbs of Moon, for the boundary to have the observed width at a distance of  $2 R_m$  from the limb, a proton gyrodiameter must be comparable to the boundary width. The gyrodiameter of a  $10^5$  °K proton in a 5-gamma field is 200 km. Since the diameter increases as the square root of the temperature, a 1000-km gyrodiameter would represent  $2.5 \times 10^6$  °K protons, or, alternatively, protons, released at rest with respect to Moon, in a solar-wind plasma having a bulk velocity of 250 km/sec.

In the second limiting case, since the distance from the limb to the spacecraft at the boundary averages  $2.0 R_m = 3480$  km, if the boundary is to spread to 1000-km thickness at this distance, the ratio of thermal velocity  $v_{||}$  to the solar-wind velocity must be 0.5:3.48. Thus, for a 400-km/sec bulk velocity, the parallel ion temperature must be

$$T_{||} = mv_{||}^2 / 3k = 1.3 \times 10^5 \text{ °K}$$

where  $v_{||}$  is 57 km/sec.

In four cases the boundary is marked also by a very sharp decrease in field, lasting 36 to 48 seconds. In two such cases, the shorter decrease is in the center of a longer decrease that we discussed earlier; in the other two, the shorter decrease appears alone (one of the latter pair appears in Fig. 3). A

characteristic duration of 42 seconds represents a width of 56 km, which, as a gyrodiameter, yields temperatures of  $(eBr)^2/3mk = 7 \times 10^3$  °K for protons, and  $1.3 \times 10^7$  °K for electrons, where  $e$  and  $m$  are the particles' charge and mass, respectively, and  $r$  is the gyro-radius. For the present we assume that the variability in this phenomenon is connected with the kinetics of the solar wind; more specific conclusions await further measurements.

Values of the 3-hour  $K_p$  index for the two featureless examples in Fig. 3 are 0+ and 0<sub>0</sub>;  $K_p$  averages 2<sub>0</sub> for the 15 passes that exhibit diamagnetic effects. This correlation, if confirmed by further data, suggests that the product  $n(T_e + T_i)$ , contributing to the diamagnetic effect, is higher when geomagnetic activity is greater. A conclusive relation of the  $nT$  product to  $K_p$  has not been published;  $K_p$  and  $T$  tend to increase with increase in velocity (4-6), while published correlations of velocity with density imply decreased or constant density with increase in  $K_p$  (5, 6). Moreover Mariner-II data (5) show that the product  $n(T_e + T_i)$ , at 1 astronomical unit, can vary at least over the range  $1.4 \times 10^{11}$  to  $2.0 \times 10^{13}$  °K/m<sup>3</sup> [ $T_e = 2T_i$  is assumed (7)]. Consequently, the increase of  $B_2$  above the interplanetary  $B_1$  of 6 gamma (Fig. 3), inferred from the plasma equation of motion, could be as small as 0.3 gamma; such a small effect would be impossible to detect in view of the fluctuations present and the paucity of available data. Finally, the occurrence of the dips at higher  $K_p$  values indicates that edge effects, creating a plasma layer, may be sensitive to the bulk velocity.

A bound on the length of the lunar cavity follows from Dessler (8), who defines the maximum tangent of the angle of closure as the magnetoacoustic velocity divided by the bulk velocity. Thus, assuming no pressure within the cavity, the minimum length is  $5.7 R_m$  for solar-wind and magnetoacoustic velocities of 400 and 70 km/sec, respectively. As the aposelene of Explorer 35 moves toward the lunar antisolar direction because of the Earth-Moon motion about Sun, measurements defining the length of the cavity may be possible.

Our preliminary assessment of these data shows no evidence of the existence of a lunar bow shock wave; thus we infer that the unipolar current system, that can flow in response to the interaction with the interplanetary magnetic

field, is strongly quenched for Moon (9). This inference implies in turn that the effective impedance presented by Moon to the solar wind is so great as to limit the current magnitude to a level at which the induced magnetic field cannot influence significantly the flow of solar wind. The interplanetary magnetic field may be said (10) to diffuse through Moon with a Cowling time comparable to the transit time of the solar wind past Moon, so that formation of a lunar magnetosphere is inhibited. The measurements imply that contact between the solar-wind ions and the surface is complete, and the induced magnetic field of planetary scale within Moon is insufficient to deviate appreciably the flow of plasma.

For an electrically homogeneous Moon the lack of a strong interaction presupposes a bulk conductivity lower than about  $10^{-6}$  mho/m for an interplanetary field strength of 5 gamma (9). However, an electrically inhomogeneous Moon, with a very resistive crustal layer (as might form even for a hot body in radiative equilibrium with space), would suffice to quench the unipolar current system in a manner consistent with our negative findings. Therefore attempts to determine an interior temperature regime based on the relation of temperature to electrical conductivity are premature.

D. S. COLBURN, R. G. CURRIE  
J. D. MIHALOV, C. P. SONETT  
*Space Sciences Division,  
Ames Research Center,  
Moffett Field, California*

#### References and Notes

1. C. P. Sonett, D. S. Colburn, R. G. Currie, *J. Geophys. Res.*, in press.
2. H. Alfvén and C.-G. Fälthammar, *Cosmical Electrodynamics* (Oxford Univ. Press, Oxford, ed. 2, 1963), pp. 203-08.
3. W. R. Smythe, *Static and Dynamic Electricity* (McGraw-Hill, New York, ed. 2, 1950), pp. 65-68.
4. C. W. Snyder, M. Neugebauer, U. R. Rao, *J. Geophys. Res.* **68**, 6361 (1963).
5. M. Neugebauer and C. W. Snyder, *ibid.* **71**, 4469 (1966).
6. J. M. Wilcox, K. H. Schatten, N. F. Ness, *ibid.* **72**, 19 (1967).
7. J. H. Wolfe, R. W. Silva, D. D. McKibbin, *Trans. Amer. Geophys. Union* **48**, 182 (1967).
8. A. J. Dessler, *J. Geophys. Res.* **69**, 3913 (1964).
9. C. P. Sonett and D. S. Colburn, *Nature* **216**, 340 (1967).
10. T. Gold, in *The Solar Wind*, R. J. Mackin, Jr., and M. Neugebauer, Eds. (Jet Propulsion Lab., Pasadena, 1966), pp. 381-91.
11. We thank our colleagues in the Anchored Interplanetary Monitoring Platform project office, Goddard Space Flight Center, for their untiring efforts in our behalf; and Messrs. Longland, Pearlstein, and Morrisette (Honeywell Radiation Center) for making this experiment a success. We also acknowledge helpful discussions with S. H. Ward, J. R. Spreiter, and D. L. Webster. One of us (R.G.C.) is a NAS postdoctoral resident research associate.

11 September 1967; revised 23 October 1967